Geophysical Research Letters®

Key Points:

- Moisture availability in Asian dust source regions to the North Pacific Ocean were controlled by precession
- North Pacific dust flux reveals dominant obliquity variations, but is out-of-phase at different latitudes
- The westerlies in the Northern Hemisphere were primarily modulated by obliquity cycles in the late Pleistocene

Supporting Information:

Supporting Information may be found in the online version of this article.

Correspondence to:

H. Yang and Q. Liu,
yanghu@sml-zhuhai.cn;
qsliu@sustech.edu.cn

Author Contributions:

Data curation: Juan C. Larrasoaña, André Bahr, Xun Gong, Yanan Zhang
Formal analysis: Yanguang Liu, Qiuzhen Yin, Peter D. Clift, Stefanie Kaboth-Bahr
Funding acquisition: Qingsong Liu
Investigation: Yanguang Liu, Stefanie Kaboth-Bahr, André Bahr
Methodology: Xun Gong
Project administration: Qingsong Liu
Resources: André Bahr
Software: Yi Zhong, Qiuzhen Yin, Xun Gong
Supervision: Hu Yang
Validation: Peter D. Clift, Xun Gong
Visualization: Hu Yang, David J. Wilson, Samuel L. Jaccard

Orbital Controls on North Pacific Dust Flux During the Late Quaternary

Yi Zhong[1] [iD], Yanguang Liu[2] [iD], Hu Yang[3,4] [iD], Qiuzhen Yin[5] [iD], David J. Wilson[6] [iD], Zhengyao Lu[7] [iD], Samuel L. Jaccard[8] [iD], Torben Struve[9] [iD], Peter D. Clift[6,10] [iD], Stefanie Kaboth-Bahr[11], Juan C. Larrasoaña[12,13,14] [iD], André Bahr[15] [iD], Xun Gong[16,17,18], Debo Zhao[19] [iD], Yanan Zhang[1] [iD], Wenyue Xia[1], and Qingsong Liu[1,20,21]

[1]Department of Ocean Science and Engineering, Centre for Marine Magnetism (CM²), Southern University of Science and Technology, Shenzhen, China, [2]Key Laboratory of Marine Geology and Metallogeny, First Institute of Oceanography, Ministry of Natural Resources (MNR), Qingdao, China, [3]Southern Marine Science and Engineering Guangdong Laboratory, Zhuhai, China, [4]Alfred Wegener Institute, Helmholtz Centre for Polar and Marine Research, Bremerhaven, Germany, [5]Earth and Climate Research Center, Earth and Life Institute, Université catholique de Louvain, Louvain-la-Neuve, Belgium, [6]Department of Earth Sciences, University College London, London, UK, [7]Department of Physical Geography and Ecosystem Science, Lund University, Lund, Sweden, [8]Institute of Earth Sciences, University of Lausanne, Lausanne, Switzerland, [9]Marine Isotope Geochemistry, Institute for Chemistry and Biology of the Marine Environment (ICBM), University of Oldenburg, Oldenburg, Germany, [10]Department of Geology and Geophysics, Louisiana State University, Baton Rouge, LA, USA, [11]Institute of Geological Sciences, Free University Berlin, Berlin, Germany, [12]IGME, CSIC, Zaragoza, Spain, [13]Department of Science, Universidad Pública de Navarra, Pamplona, Spain, [14]Institute for Advanced Materials and Mathematics INAMAT², Universidad Pública de Navarra, Pamplona, Spain, [15]Institute of Earth Sciences, Heidelberg University, Heidelberg, Germany, [16]Institute for Advanced Marine Research, China University of Geosciences, Guangzhou, China, [17]State Key Laboratory of Biogeology and Environmental Geology, Hubei Key Laboratory of Marine Geological Resources, China University of Geosciences, Wuhan, China, [18]Shandong Provincial Key Laboratory of Computer Networks, Qilu University of Technology (Shandong Academy of Sciences), Jinan, China, [19]Key Laboratory of Marine Geology and Environment, Institute of Oceanology, Chinese Academy of Sciences, Qingdao, China, [20]Southern Marine Science and Engineering Guangdong Laboratory (Guangzhou), Guangzhou, China, [21]Shanghai Sheshan National Geophysical Observatory, Shanghai, China

Abstract Airborne mineral dust is sensitive to climatic changes, but its response to orbital forcing is still not fully understood. Here, we present a reconstruction of dust input to the Subarctic Pacific Ocean covering the past 190 kyr. The dust composition record is indicative of source moisture conditions, which were dominated by precessional variations. In contrast, the dust flux record is dominated by obliquity variations and displays an out-of-phase relationship with a dust record from the mid-latitude North Pacific Ocean. Climate model simulations suggest precession likely drove changes in the aridity and extent of dust source regions. Additionally, the obliquity variations in dust flux can be explained by meridional shifts in the North Pacific westerly jet, driven by changes in the meridional atmospheric temperature gradient. Overall, our findings suggest that North Pacific dust input was primarily modulated by orbital-controlled source aridity and the strength and position of the westerly winds.

Plain Language Summary Glacial-interglacial climate variations can affect dust transport to the ocean, but the controls on past dust fluxes to the North Pacific Ocean remain poorly constrained. This region is important because fertilization of phytoplankton growth by dust-borne iron may have contributed to lower glacial atmospheric CO_2, and dust records could also constrain the past dynamics of the North Pacific westerly winds. Here, we highlight the dominance of obliquity cycles in modulating latitudinal shifts of the westerly winds and, in turn, dust inputs. In contrast, precession regulates the aridity of the dust source regions, which determines both dust emission rates and composition. Such orbital-scale fluctuations in the dust flux could influence ocean-atmosphere interactions in the middle and high northern latitudes, with implications for global atmospheric circulation and ocean carbon storage.

1. Introduction

Eolian dust is an important component of the Earth's climatic system that affects the radiative balance, precipitation processes, and the functioning of terrestrial and marine ecosystems (Jickells et al., 2005; Shao et al., 2011; Tagliabue et al., 2017). In the Northern Hemisphere, dust is primarily sourced from North Africa, the Middle East,

Writing – original draft: Yi Zhong, Hu Yang, Samuel L. Jaccard, Torben Struve, Peter D. Clift, Stefanie Kaboth-Bahr, Juan C. Larrasoaña, André Bahr, Debo Zhao, Yanan Zhang, Qingsong Liu

Writing – review & editing: Yi Zhong, Hu Yang, David J. Wilson, Torben Struve, Juan C. Larrasoaña, Debo Zhao, Yanan Zhang, Wenyue Xia, Qingsong Liu

as well as Central and East Asia. Dust from these source regions is transported primarily by the prevailing trade and westerly wind systems (Uno et al., 2009; Figure 1). Dust deposited at the ocean surface can also affect climate via ocean fertilization because the iron released from partial mineral dissolution can increase primary productivity and thus carbon uptake, thereby affecting atmospheric CO_2 concentrations (Martin, 1990; Moore et al., 2013). Moreover, cloud-aerosol interactions in the atmosphere remain a major uncertainty in climate model simulations and predictions (Szopa et al., 2021). Thus, improving our understanding of the mechanisms that control dust mobilization, atmospheric transport, and deposition in response to climate forcing may enhance our ability to project future changes in these systems (Kok et al., 2023).

Variability in eolian dust deposition in the North Pacific Ocean can be attributed to multiple factors, including dust emissions associated with the availability and supply of fine sediments (from fluvial or glacial sources), dust emission and transport efficiency (related to wind velocity), and the mode of deposition (dry vs. wet deposition) (Maher et al., 2010; Mayaud et al., 2016). For example, both high and low temperatures, as well as dry and wet climatic conditions, have been related to the formation of sandstorms and sand transport (Mao et al., 2011; Yang et al., 2019). Moreover, the Northern Hemisphere westerly winds play an important role in mid-to high-latitude atmosphere-ocean coupling (Zhang et al., 2006; Figure 1), exerting considerable influence on weather patterns and precipitation variability (Shaw et al., 2016; Uno et al., 2009). The temporal evolution of the position and intensity of the westerlies also affects the migration of the summer rainfall belt over East Asia (Chiang et al., 2015, 2017) (Figure S1 in Supporting Information S1), as well as the precipitation regime over the arid lands of Central Asia (Zhao et al., 2014). The westerlies dominate the transport of Central Asian dust from land to sea in this region, such that changes in dust provenance or fluxes may reflect changes in the westerly wind system.

Previous studies have investigated mid-latitude atmospheric circulation and dust-climate interactions from various perspectives. Modern observations reveal that the Northern Hemisphere westerlies have experienced a poleward shift in response to global warming, which is attributable to the expansion of the tropics associated with changes in meridional temperature gradients (Chen et al., 2020; Yang, Lohmann, Krebs-Kanzow, et al., 2020). Beyond the relatively limited era of instrumental records, reconstructions of westerly winds in the Northern Hemisphere based on proxy records have primarily focused on the last glacial-interglacial transition (Gray et al., 2020; Herzschuh et al., 2019; Nagashima et al., 2007, 2011). During the late Quaternary, reconstructions from dust proxies in the North Pacific Ocean indicate higher fluxes during glacial periods than during interglacial periods. This pattern has been linked in part to the enhancement of Asian aridification during glacial stages (Hovan et al., 1989; Jacobel et al., 2017). Over longer geological timescales, latitudinal migrations of the westerlies have predominantly been attributed to variations in Plio-Pleistocene meridional temperature gradients and ice volume (Abell et al., 2021; Zhong et al., 2022). However, our understanding of the overall dynamics of the westerlies with regard to dust emission and transport in this region remains incomplete, especially on orbital timescales, because of a lack of high-resolution dust records from the North Pacific Ocean that extend beyond the Last Glacial Maximum (Nagashima et al., 2007). In addition, the majority of previous studies focused on the southern margin and the meteorological core of the westerly wind belt (Abell et al., 2023), while the northern margin of the westerlies has remained sparsely studied (Serno et al., 2017), limiting a comprehensive understanding of the westerly wind dynamics and dust transport on orbital timescales.

In this study, we present a new high-resolution eolian dust record spanning the past 190 kyr based on sediments from gravity Core LV63-4-2 that was recovered from the slopes of Detroit Seamount in the Subarctic Pacific Ocean (Zhong et al., 2020, 2021; Figure 1). Both precession- and obliquity-paced dust fluctuations are identified in this record. By synthesizing multiple proxies and combining them with climate simulations conducted under different orbital configurations, we propose that the precession- and obliquity-paced dust fluctuations can be attributed to changes in aridity in the dust source regions and the migration/intensity of the westerly winds, respectively.

2. Materials and Methods

This study is based on gravity Core LV63-4-2 (51.63°N, 167.81°E; 2,946 m water depth), which was collected from the northern Emperor Seamounts in the western subarctic Pacific Ocean during a Russian-Chinese joint expedition on R/V *Akademik M.A. Lavrentyev* in 2013 (Figure 1). The 6.88 m long sediment sequence is dominated by fine-grained silt and clay, with occasional volcanic ash layers. The age model for Core LV63-4-2 is based on six AMS ^{14}C dates (for the upper part) in combination with planktonic foraminiferal oxygen isotope
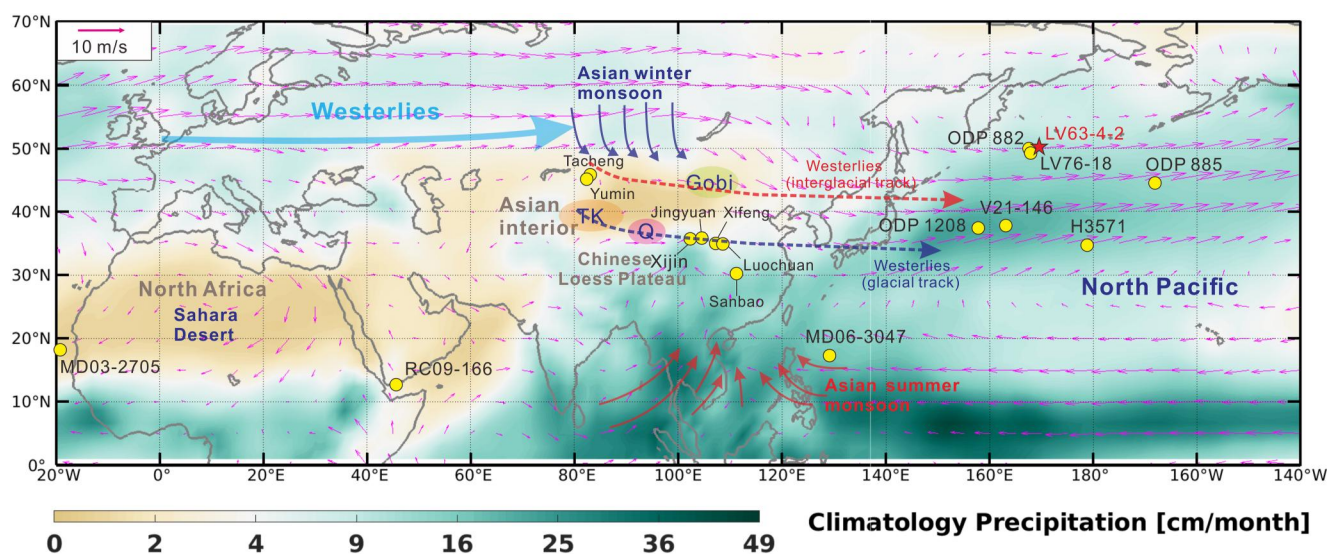
Figure 1. Regional map showing annual mean precipitation (color shading; see scale bar) and 850 hPa winds (arrows), based on the NCEP-DOE reanalysis (1979–2020) (Kanamitsu et al., 2002). Marine records include core LV63-4-2 (this study), core LV76-18 (Cheng et al., 2022), ODP Site 882 (Serno et al., 2017), ODP Site 1208 (Abell et al., 2023), ODP Site 885 (Zhang, Liu, et al., 2020), core V21-146 (Hovan et al., 1989), and core H3571 (Kawahata et al., 2000) in the North Pacific, core MD06-3047 in the western Philippine Basin (Xu et al., 2015), core MD03-2705 in the east Atlantic (Skonieczny et al., 2019), and core RC09-166 in the Gulf of Aden (Tierney et al., 2017). Terrestrial records include the loess sequences from Jingyuan (Sun et al., 2019), Xijin (Guo et al., 2022), Xifeng (Guo et al., 2009), Luochuan (Han et al., 2020), Tacheng, and Yumin (Li et al., 2019b), and speleothem records from Sanbao (Cheng et al., 2016). The light blue arrow depicts the general direction of the westerly winds. Red and dark blue dashed arrows qualitatively indicate the dominant position of the westerly winds during interglacial and glacial periods of the Quaternary, respectively (Abell et al., 2021; Kapp et al., 2011). Red and dark blue solid arrows indicate the Asian summer monsoon and Asian winter monsoon, respectively. Major Asian dust sources are also indicated: Gobi Desert (Gobi), Taklimakan Desert (TK), and Qaidam Basin (Q).

stratigraphy, paleomagnetic events, tephrochronology, and the correlation of sediment lightness proxy data to carbonate content data from Ocean Drilling Program (ODP) Site 882 (Jaccard et al., 2010; Liu et al., 2022; Zhong et al., 2020, 2021) (Figure S2 in Supporting Information S1).

In this study, we used the upper 6.2 m of core LV63-4-2 to generate a continuous record of hematite (Hm) and goethite (Gt) content for the last ~190 kyr, when there was an average sedimentation rate of ~3.3 cm/kyr. Sampling resolution was 0.6 kyr. We used diffuse reflectance spectroscopy (DRS) measurements to obtain a record of the combined relative concentration of Hm and Gt (Rel$_{Hm + Gt}$) (Zhang et al., 2018), which is presented per unit mass of dry sediment (details of the experimental procedures are given in Text S1 in Supporting Information S1). To determine the input history of a given sedimentary component, we define the Rel$_{Hm + Gt}$ flux to reflect Hm and Gt inputs: Flux of Rel$_{Hm + Gt}$ = Rel$_{Hm + Gt}$ × DBD × LSR × (100-CaCO$_3$%-Opal%-TOC%) × dust fraction (DBD, dry bulk density; LSR, linear sedimentation rate) (Koffman et al., 2021; Liu et al., 2022; Yao et al., 2022).

Relative proportions of sedimentary hematite and goethite (Hm/(Hm + Gt)) provide a proxy for source aridification, with higher Hm/(Hm + Gt) ratios corresponding to more arid conditions, or at least greater seasonality (Clift et al., 2014; Lepre & Olsen, 2021; Limmer et al., 2012).

We also conducted spectral analyses to examine the periodicities in the Hm/(Hm + Gt), Rel$_{Hm + Gt}$, and Rel$_{Hm + Gt}$ flux records. All data were linearly interpolated at 1 kyr spacing and detrended before analysis. The analysis was performed using the *REDFIT* spectral analysis program in the *Past 3.0* software package. We also applied Gaussian band-pass filters to the eolian dust records with the Acycle software (Li et al., 2019a) in order to extract oscillations associated with the precession and obliquity periods, using filters centered at 0.0476 ky^{-1} (21-kyr cycle) and 0.02439 kyr^{-1} (41-kyr cycle), respectively.

Using the Alfred Wegener Institute Earth System Model (AWI-ESM; Sidorenko et al., 2019), we conducted two sets of simulations to examine the physical mechanisms potentially controlling the dust fluctuations in our record. The AWI-ESM has been validated and widely used in climate change studies over different timescales (Lohmann

et al., 2020; Shi et al., 2020; Yang, Lohmann, Krebs-Kanzow, et al., 2020). The details of the climate model simulations are provided in Text S2 in Supporting Information S1.

3. Results

We determined the hematite and goethite contents in Core LV63-4-2 to assess variations in the $Rel_{Hm + Gt}$ (Figure 2e), the $Rel_{Hm + Gt}$ flux (Figure 2f), and the Hm/(Hm + Gt) ratio (Figure 2d) over the past 190 kyr. In general, the flux of $Rel_{Hm + Gt}$ (Figure 2f) is in-phase with the variations in $Rel_{Hm + Gt}$ (Figure 2e), which suggests that any changes in accumulation rate related to inputs of other sediment components did not bias the signal in the $Rel_{Hm + Gt}$ record.

Despite some similarities during glacial times associated with Marine Isotope Stages (MIS) 2, 4, 5b, 5d, and 6 (Figure 2), the Hm/(Hm + Gt), $Rel_{Hm + Gt}$, and flux of $Rel_{Hm + Gt}$ records show different spectral patterns (Figure 3). Variations of Hm/(Hm + Gt) in Core LV63-4-2 have prominent power in the precession band ($\sim$19–23 kyr cycles) (Figures 3a and 3b). In contrast to the Hm/(Hm + Gt) record, the orbital-scale variability in the $Rel_{Hm + Gt}$ in Core LV63-4-2 does not show a clear precession signal, and instead is dominated by a 41-kyr obliquity cycle (Figures 3c and 3d). It is also noteworthy that a 41-kyr obliquity cycle is evident, but less strongly expressed, in variations of Hm/(Hm + Gt) in Core LV63-4-2 (Figures 3a and 3b). Spectral and wavelet analysis of the $Rel_{Hm + Gt}$ flux record reveals a combination of both precession and obliquity components (Figures 3e and 3f).

4. Discussion

4.1. Hematite and Goethite as Proxies for Eolian Input in North Pacific Marine Sediments

Eolian dust in marine sediments contains abundant Hm and Gt that are derived from weathering and erosion processes in the neighboring subtropical drylands where most atmospheric dust is produced (Larrasoaña et al., 2015; Liu et al., 2012; Oldfield et al., 2014). Hematite and Gt are more stable than other ferromagnetic minerals in a variety of sedimentary environments, implying that they can provide valuable records of eolian input to the marine environment (Lepre & Olsen, 2021; Liu et al., 2012). Hematite is preferentially associated with drier, hotter, or more seasonal conditions, whereas Gt is formed in cooler, wetter climates (Clift et al., 2014; Lepre & Olsen, 2021; Limmer et al., 2012). The Hm and Gt abundances and their relative ratios have previously been used as proxies to document the supply of eolian dust to North Pacific pelagic sediments (Zhang et al., 2018). Specifically, North Pacific Ocean sediments have been shown to contain eolian Hm and Gt particles (Maher, 2011; Yamazaki, 2009; Zhang et al., 2018, 2020) that were transported by the westerlies from the drylands of Central Asia to distal locations in the North Pacific Ocean at latitudes of up to 50°N (Maher, 2011; Serno et al., 2014).

Other than eolian dust, our studied pelagic sediments are also influenced by the supply of biogenic, terrigenous, and volcanogenic particles. Given the location of Core LV63-4-2, on a topographic high of the northern Emperor Seamount chain and in a distal position from the Asian continent, the influence of riverine and submarine mass flows on Hm and Gt abundances is expected to be negligible. Furthermore, most magnetic particles derived from continental sources other than dust appear to be dominated by ferromagnetic particles rather than by antiferromagnetic Hm and Gt (Lund et al., 2021).

However, Hm and Gt have been reported in volcanogenic glacial sediments and ash samples from Alaska, albeit in much lower concentrations than seen in Asian dust (Koffman et al., 2021; Nwaodua et al., 2014; Ortiz et al., 2009). Such glacial sediments and ash can also be transported over long distances by ice rafting and ocean currents (Caissie et al., 2016; Lund et al., 2021; Nwaodua et al., 2014). Our geochemical data show that the detrital component in Core LV63-4-2 sediments derives from binary mixing between Asian dust and circum-Pacific volcanogenic material (Text S3 and Figure S3 in Supporting Information S1) (Weber et al., 1996; Zhang et al., 2016). We followed the thorium-based mass balance approach of Serno et al. (2014) to calculate the relative proportions of Asian dust and volcanogenic material in Core LV63-4-2 (Text S4 and Figure S4 in Supporting Information S1). The Hm and Gt content is about one order of magnitude higher in Asian dust than in volcanogenic material (Koffman et al., 2021) (Figure S4b and S4c in Supporting Information S1), so the eolian input from East/Central Asian dust sources appears to dominate the Hm and Gt signals in Core LV63-4-2. This conclusion is further supported by the similarity of the $Rel_{Hm + Gt}$ record to nearby records of [4]He-based
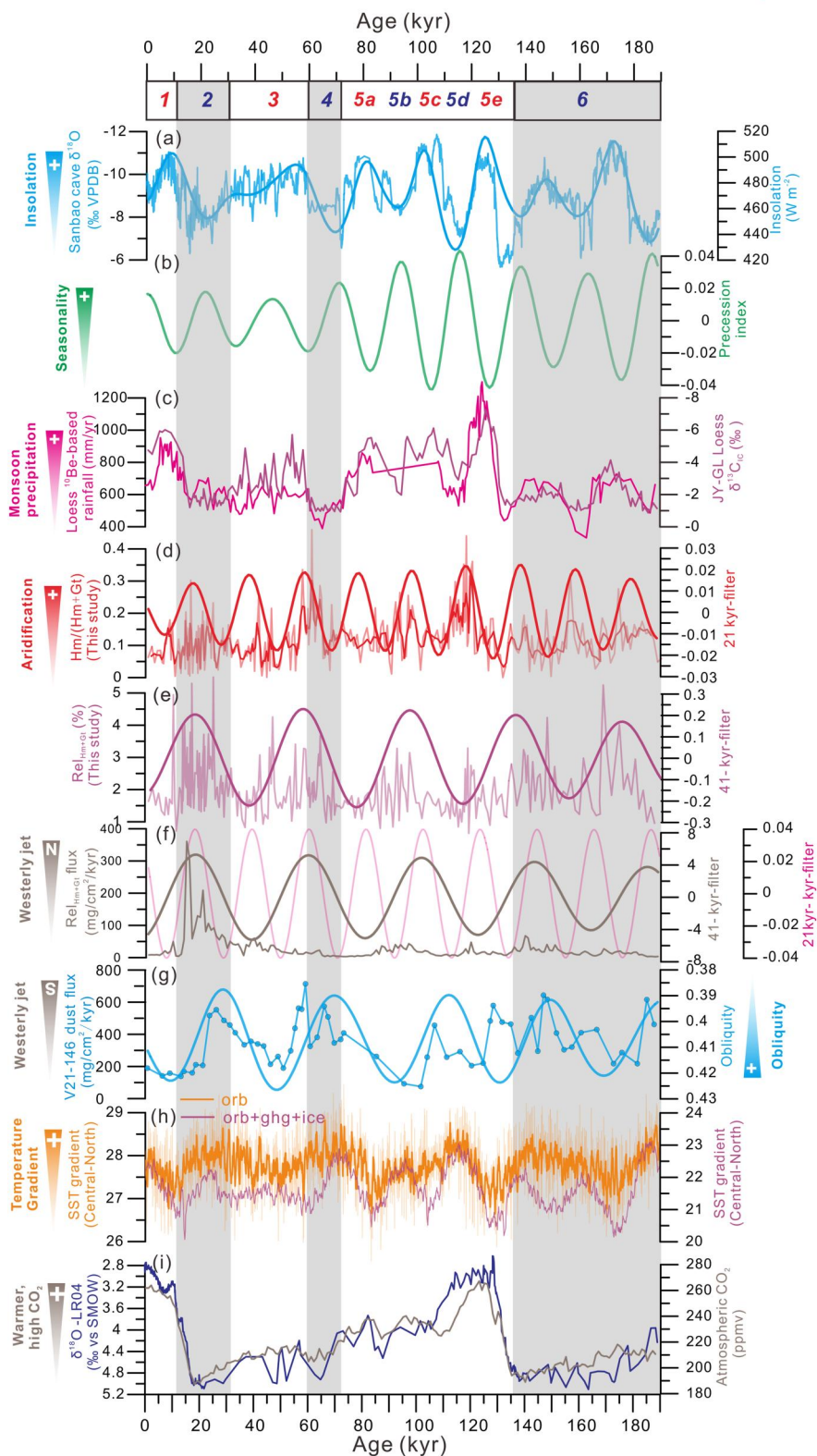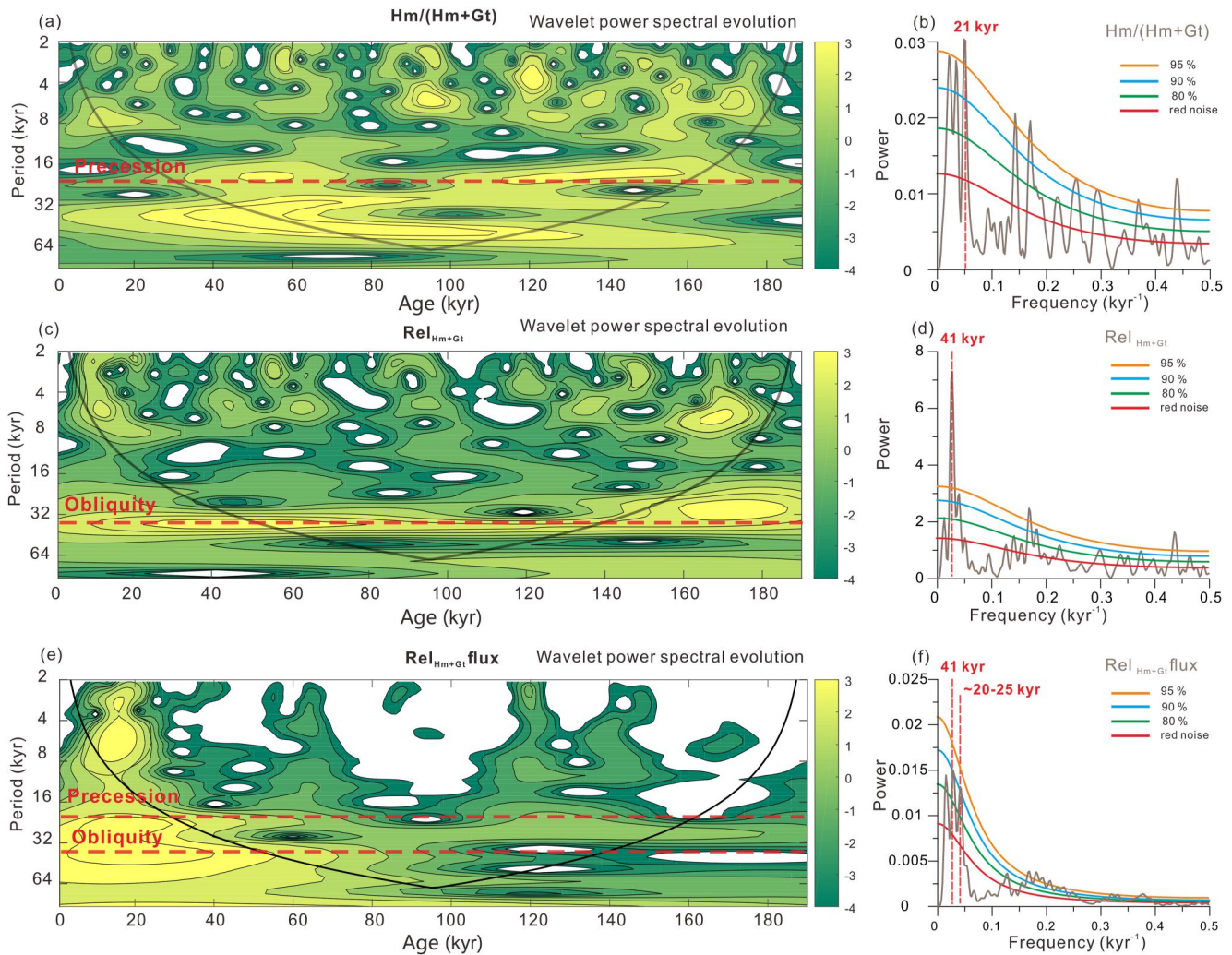
Figure 2.

Figure 3. Wavelet power spectra of (a) Hm/(Hm + Gt) ratio, (c) $Rel_{Hm + Gt}$ content, and (e) $Rel_{Hm + Gt}$ flux in core LV63-4-2. Solid black contour lines identify regions where spectral power meets the 5% significance level against red noise. The thick line identifies the cone of influence where edge effects could impact the signal. Red dashed lines represent the major periods of precession (19–23 kyr) and obliquity (41 kyr). Power spectrum analysis of (b) Hm/(Hm + Gt) ratio, (d) $Rel_{Hm + Gt}$ content, and (f) $Rel_{Hm + Gt}$ flux in core LV63-4-2. Red, green, blue, and orange lines represent theoretical red noise, 80%, 90%, and 95% false-alarm levels, respectively. Red dashed lines indicate significant peaks at periods of 21 kyr, ∼20–25 kyr, and 41 kyr.

terrigenous fluxes recorded at ODP Site 882 (Serno et al., 2017) (Figure S5e in Supporting Information S1) and black soot content in Core LV76-18 (Cheng et al., 2022) (Figure S5e in Supporting Information S1). As such, we consider Hm and Gt abundances reliable proxies for Asian dust supply to the North Pacific (Maher, 2011), even in depositional environments that are dominated by volcanogenic detritus.

Figure 2. Eolian dust and rainfall records from the Asian continental interior and Pacific Ocean since 190 kyr. (a) Chinese cave stalagmite $\delta^{18}O$ from Sanbao (Cheng et al., 2016) and Northern Hemisphere summer insolation (65°N, July-September) (Laskar et al., 2004); (b) Precession index (Laskar et al., 2004); (c) Reconstructed East Asian monsoon precipitation in its northern region based on records of ^{10}Be in loess (Beck et al., 2018) and $\delta^{13}C$ of loess carbonate (Sun et al., 2019); (d) Hm/(Hm + Gt) ratio (original data and three-point filter) in core LV63-4-2, and 21 kyr Gaussian bandpass filtered output (thick red line); (e) $Rel_{Hm + Gt}$ content (original data and three-point filter) in core LV63-4-2, and 41 kyr Gaussian bandpass filtered output (thick purple line); (f) $Rel_{Hm + Gt}$ flux (mg/cm^2/kyr, gray line) in core LV63-4-2, 41 kyr (thick gray line) and 21 kyr (thick pink line) Gaussian bandpass filtered output; (g) Dust flux record from core V21-146 on Shatsky Rise (Hovan et al., 1989) (line with symbols), and obliquity index (Laskar et al., 2004) (inverse scale); (h) Modeled sea surface temperature (SST) gradient (Central (160°E−180°E, 20°N−30°N)–North (160°E−180°E, 45°N−55°N)) in the North Pacific Ocean during the last 190 kyr for ORB + GHG + ICE and ORB experiments (see Text S2 in Supporting Information S1); (i) LR04 benthic $\delta^{18}O$ stack (Lisiecki & Raymo, 2005) and atmospheric CO_2 concentrations from EPICA Dome C ice core (Lüthi et al., 2008). Gray bars indicate glacial periods, and all periods are labeled with marine isotope stage (MIS) numbers.

4.2. Precession Control on the Moisture Conditions in Dust Source Regions

Precession forcing is recognized as a pacemaker of low-latitude climate change and in particular, as a driver of variability in the hydrological cycle (Huang et al., 2020; Wang, 2021) (Figures 2a and 2b). Such a control is also recorded here in the changes in the Hm/(Hm + Gt) ratio and dust flux records (Figures 2d–2f). Previous studies suggest that precessional changes influence the near-surface wind intensity (Evan et al., 2016; Kang et al., 2022; Wu et al., 2022) and/or source moisture content (Maher et al., 2010; Mayaud et al., 2016; Újvári et al., 2017), thereby controlling dust emissions in the source areas and thus the dust fluxes to Core LV63-4-2.

A clear precession signal is recorded in the loess deposits of Central Asia (Cheng et al., 2020, 2021; Li et al., 2019b) and on the Chinese Loess Plateau (Guo et al., 2022). In contrast, long-term aridity records from the Taklimakan Desert/Tarim Basin display 100-kyr cycles in the late Quaternary and lack a strong precession signal (Fang et al., 2020; Liu et al., 2020). Some climatic modeling simulations indicate that precession forcing is the dominant factor controlling the differences in moisture patterns between Central and East Asia, with out-of-phase relationships between these two regions (Li et al., 2020). This finding is attributed to different expressions of orbital forcing on spatial variability and different sensitivities to high- and low-latitude forcing. Moreover, Cheng et al. (2021) used numerical modeling experiments and optically stimulated luminescence ages from Central Asia to argue that dust accumulation during the Last Glacial Maximum showed an anti-phase relationship with Northern Hemisphere summer insolation at 65 °N, which is modulated by precession (Berger & Loutre, 1991). This relationship could be explained by the increased extent of the Northern Hemisphere ice sheets, which would have enhanced the intensity of the Siberian High (Xie et al., 2019). In such a scenario, more frequent, strong, near-surface winds would be an important factor responsible for the Asian dust export.

In addition, environmental conditions in the source areas can also produce large variations in sediment supply. For example, changes in vegetation cover and soil moisture influence the availability of fine material in the potential dust source areas (de Menocal et al., 2000; Wu et al., 2022). This relationship is evidenced by the link between low $\delta^{13}C$ values (reflecting C3 vs. C4 vegetation in the source region) in the absolute-dated Gulang Loess sequence (Sun et al., 2019) and the high ^{10}Be content in the Xifeng Loess over precessional timescales (Beck et al., 2018; Figure 2c). Monsoon precipitation records from the Xijin drill cores on the western Chinese Loess Plateau have also revealed dominant 23-kyr cycles through both interglacial and glacial periods, consistent with local precessional insolation forcing (Guo et al., 2022; Figure 2a). Increased humidity during warm periods in the dust source areas would have promoted vegetation growth, thereby reducing the production of dust and its subsequent entrainment (Li et al., 2019c). As a corollary, increased dust inputs during cool periods (Figure 2f) were closely related to decreased summer precipitation (Figure 2d). We further recognize that seasonal increases in precipitation and fluvial activity could have enhanced sediment availability and promoted dust generation in East/Central Asia (Li et al., 2019c).

A precessional control over dust fluxes arising from precipitation in the source regions is further demonstrated by climate model simulations exploring the regional sensitivity of summer precipitation in the Asian-African region to precession (Text S5 in Supporting Information S1, Figure 4a). Those results are consistent with a dominant control of precession forcing on summer precipitation in North China (Lyu & Yin, 2022; Lyu et al., 2021) and North Africa (Larrasoaña et al., 2015; Skonieczny et al., 2019) (Figure S5d in Supporting Information S1). Wetter conditions in dust source regions could reduce the production and supply of dust, thereby contributing to decreased dust fluxes during intervals of strong precession-driven insolation (Figure 4a). This precession signal was also previously found in the loess sequence in the Tacheng Basin of eastern Central Asia (Li et al., 2019b; Figure 1). Conversely, weakening of the East Asian summer monsoon during precession-driven insolation minima would be expected to channel less precipitation from the tropics towards Central Asia, thereby facilitating aridification and promoting wild-fire activity, as recorded in the soot record in Core LV76-18-1 from the North Pacific Ocean (Cheng et al., 2022; Figure S5e in Supporting Information S1). Similarly, ^{230}Th-normalized dust fluxes at the West African margin (Skonieczny et al., 2019; Figure S5d in Supporting Information S1) show a high correlation with summer insolation and only limited glacial-interglacial changes, with coherent variability observed across the African monsoon belt (Tierney et al., 2017; Figure S5c in Supporting Information S1).

Since our Hm/(Hm + Gt) record reveals relatively weak variations on obliquity timescales, we examined how obliquity impacts precipitation. Model simulations with different obliquity configurations (Text S2 in Supporting
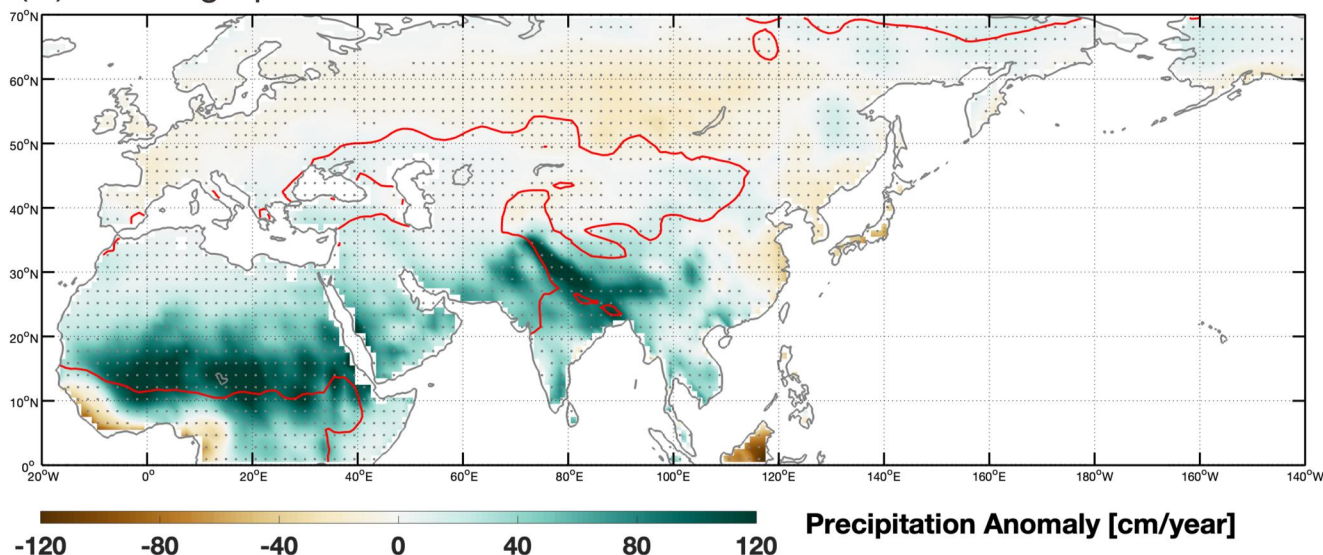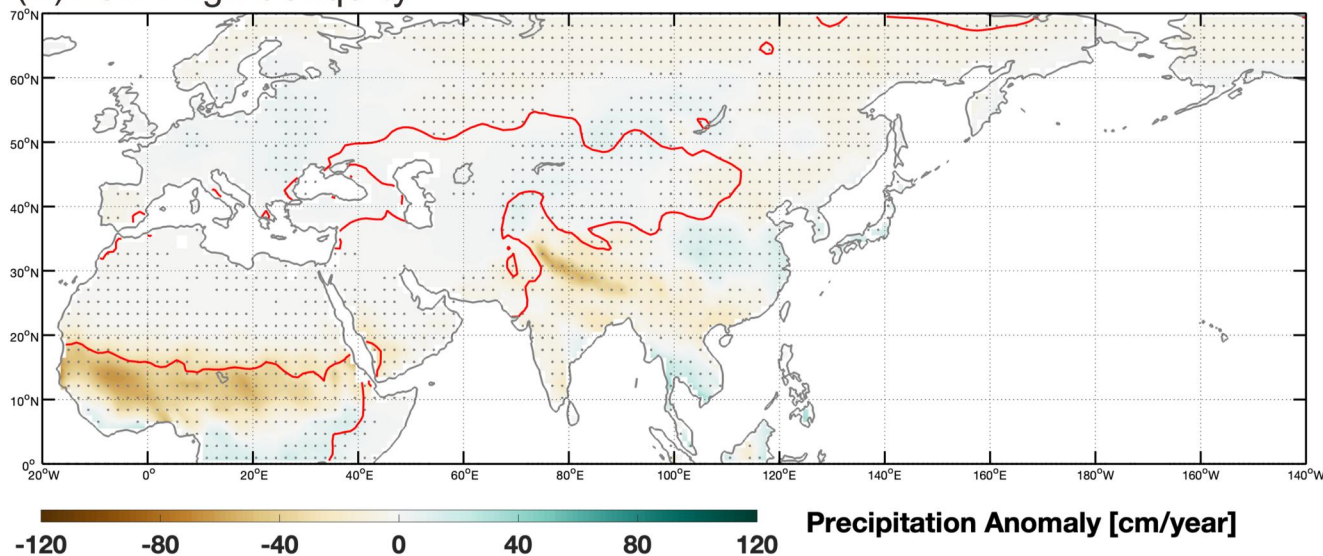
Figure 4. (a) Annual precipitation anomaly in the AWI-ESM low-precession experiment compared to the high-precession experiment. (b) Annual precipitation anomaly in the AWI-ESM low-obliquity experiment compared to the high-obliquity experiment. The arid climate zones, or dust source regions, are demarcated by the red contour lines, which represent 40 cm/year precipitation in the high-obliquity and high-precession experiments, respectively. In all cases, the plotted results are based on the last 100 years of the experiments, and stippling indicates regions where the anomalies are statistically significant (two-tailed Student's t-test).

Information S1) suggest that low obliquity reduces precipitation in the monsoon domain of Africa and Asia (Figure 4b), which would be expected to increase the aridity. Nonetheless, the contribution of obliquity changes to aridity is relatively weak when compared to the effect of precession, in particular over the relevant dust source regions.

4.3. Influence of Obliquity on Atmospheric Transport

Although precession influenced local conditions in dust source regions (e.g., North Africa, Middle East, and Centra Asia), the dust fluxes to the North Pacific display a different depositional pattern. In particular, a strong obliquity signal is seen in the dust input to Core LV63-4-2 (Text S5 in Supporting Information S1; Figures 2e, 2f, 3c and 3d). Within the obliquity band, the eolian input to the Pacific Ocean appears to be out-of-phase between high- and mid-latitudes (Figures 2f and 2g; Hovan et al., 1989). We note that this offset may be partly related to

differences in age models (Figure S2 in Supporting Information S1) or data resolution, with additional uncertainty introduced by reconstructing lithogenic input to the ocean without normalization to a constant flux proxy (Abell et al., 2021). Despite those caveats, the eolian input to Core LV63-4-2 is clearly in phase with obliquity and appears to be out of phase with the low-resolution dust input signal in Core V21-146 (Hovan et al., 1989; Figures 2f and 2g). Such systematic behavior is unlikely to result from age model uncertainties or from fundamental weaknesses of the dust input proxies used at the different locations (Serno et al., 2017). Instead, these results suggest that eolian deposition responded to obliquity cycles in the North Pacific westerly jet, highlighting a strong role for obliquity in modulating meridional temperature gradients and latitudinal shifts of the westerly winds, as previously demonstrated for the Southern Hemisphere (Ai et al., 2020).

The reconstructed dust inputs in the high- and mid-latitudes (Figures 2f and 2g) appear to be consistent with a more southward position of the westerly winds during intervals of low obliquity. We examine this hypothesis with global climate model simulations (see Materials and Methods). Low obliquity results in less insolation at high latitudes, and more insolation at low latitudes, which enhances the temperature gradient between the mid and high latitudes (Figure 5a). It is noteworthy that the effect of obliquity on solar radiation differs between summer and winter. However, in the case of low obliquity, reduced high-latitude summer insolation leads to less oceanic heat absorption and expanded sea ice cover, which can result in year-round cooling anomalies in high latitudes. The enhanced temperature gradient, in turn, forces an equatorward intensified westerly jet (Figure 5b), as also revealed by previous studies (Lee & Poulsen, 2009; Lu et al., 2010; Timmermann et al., 2014). Such latitudinal shifts of the westerly winds would leave distinct eolian depositional patterns as a function of latitude in the Northern Hemisphere (Bosmans et al., 2018; Liu, Sun, et al., 2015) (Figure 2).

In addition, the location of the pronounced meridional sea-surface temperature gradient is linked to the mid-latitude winds, such that the North Pacific subarctic front coincides with the westerly storm tracks (Gray et al., 2020; Shaw et al., 2016). Transient simulations, particularly those driven by continuous insolation changes, also reveal a robust relationship between obliquity (Figure 2g) and the meridional sea-surface temperature gradient in the northwestern Pacific Ocean (Figure 2h). Specifically, intervals of low obliquity correspond to an increase in the meridional surface air temperature gradients (Figure 5a) and an equatorward intensification of the westerly wind field (Figure 5b). In addition to the strong obliquity signal seen in mid-to high-latitude paleoclimate records, some (but not all) tropical Indo-Pacific hydroclimate records display a similar signal, suggesting that the enhanced northerly winds associated with a strong pressure gradient between the Siberian High and the Australian Low can reinforce a southward shift of the Intertropical Convergence Zone (Liu, Sun, et al., 2015; Zhang, Liu, et al., 2020, 2022). Better constraints on the migration dynamics of the high-latitude North Pacific westerly wind system during Quaternary glacial-interglacial cycles are therefore important for improving our understanding of the interactions between high- and low-latitude processes (Liu, Sun, et al., 2015).

Obliquity changes modulate the amplitude of the seasonal cycle of insolation in both hemispheres synchronously (Berger et al., 2010). As a result, obliquity forcing is also reflected in meridional shifts of the Southern Hemisphere westerly winds (Yin, 2013), which modulate the Southern Ocean upwelling intensity and contribute to regulating glacial-interglacial atmospheric CO_2 changes (Ai et al., 2020; Mantsis et al., 2014). Our simulations support such obliquity forcing of the westerly jet in both hemispheres, with the Northern Hemisphere changes related to the temperature gradient between the middle (20°N–30°N) and high latitudes (45°N–55°N) (Figures 5a and 5b). Moreover, the presence of precessional cycles in the split jet dynamics of the South Pacific westerlies (Lamy et al., 2019) indicates that orbital-scale changes of the westerly winds were not zonally homogeneous across the Southern Hemisphere. Given the difference in land-sea distribution patterns between the two hemispheres, the prevalence of both precession and obliquity signals in precipitation and dust records from the North Pacific Ocean highlights that this orbital forcing plays an important role in global dust cycles. Further studies into the orbital dynamics of the westerly winds in both hemispheres during the late Quaternary glacial-interglacial cycles should focus on understanding the mechanisms responsible for generating such heterogeneity.

5. Conclusions

We present a new high-resolution reconstruction of dust input to the Subarctic Pacific Ocean covering the last 190 kyr. The relative abundance of eolian Hm and Gt fluctuated mainly on precessional timescales, with elevated values coincident with intervals of maximum precession. In contrast, the total dust input was dominated by
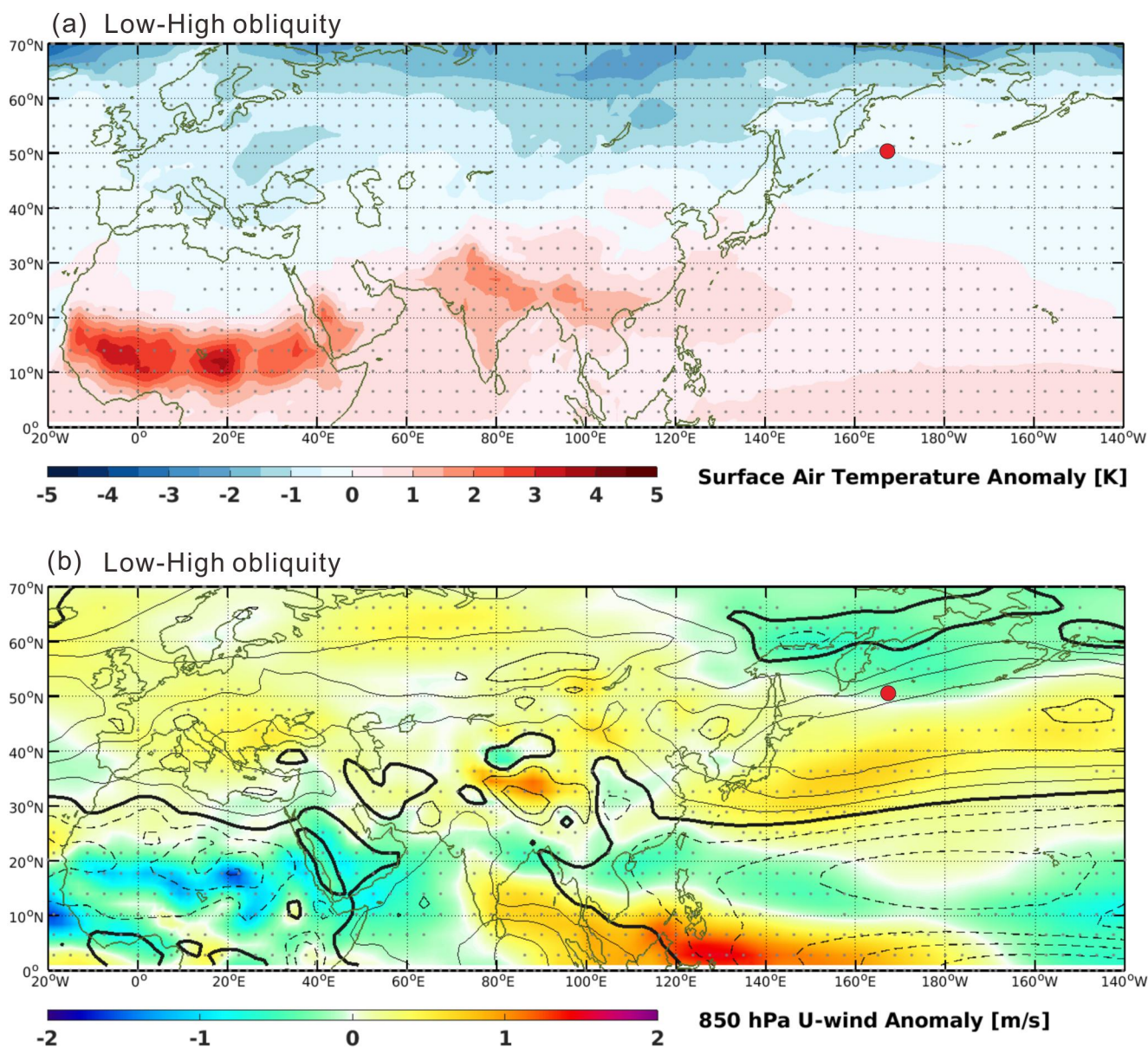
Figure 5. (a) Surface air temperature anomaly in the low-obliquity experiment compared to the high-obliquity experiment. (b) 850 hPa zonal wind anomaly in the low-obliquity experiment compared to the high-obliquity experiment. Solid lines represent westerly winds, and dashed lines represent easterly winds. An equatorward shift of the westerly winds is found in the low-obliquity experiment. In all cases, the plotted results are based on the last 100 years of the experiments, and stippling indicates regions where the anomalies are statistically significant (two-tailed Student's t-test). Red circle indicates the Core LV63-4-2 location.

obliquity variations that were out-of-phase with an existing dust record located further south. Climate model simulations suggest that the precessional fluctuations in the Hm/Gt ratio likely reflect changes in aridity in the dust source regions in response to variability in the precipitation in those regions. In addition, obliquity-driven variations in dust input can be explained by meridional shifts in the North Pacific westerly jet, causing changes in the meridional temperature gradient. These findings suggest that orbitally controlled source aridity and westerly winds both contribute to the dust input to the North Pacific Ocean.

Data Availability Statement

All data generated in this study have been deposited in the Zenodo database under the access code: https://zenodo.org/records/10252020. The AWI-ESM code is publicly available at https://fesom.de/models/awi-esm/.

References

Abell, J. T., Winckler, G., Anderson, R. F., & Herbert, T. D. (2021). Poleward and weakened westerlies during pliocene warmth. *Nature*, *589*(7840), 70–75. https://doi.org/10.1038/s41586-020-03062-1

Abell, J. T., Winckler, G., Pullen, A., Kinsley, C. W., Kapp, P. A., Middleton, J. L., et al. (2023). Evaluating the drivers of quaternary dust fluxes to the western North Pacific: East Asian dustiness and northern hemisphere gustiness. *Paleoceanography and Paleoclimatology*, *38*(9), e2022PA004571. https://doi.org/10.1029/2022PA004571

Ai, X. E., Studer, A. S., Sigman, D. M., Martínez-García, A., Fripiat, F., Thöle, L. M., et al. (2020). Southern ocean upwelling, Earth's obliquity, and glacial-interglacial atmospheric CO_2 change. *Science*, *6522*(6522), 1348–1352. https://doi.org/10.1126/science.abd2115

Beck, J. W., Zhou, W. J., Li, C., Wu, Z. K., Xian, F., Kong, X. H., & An, Z. S. (2018). A 550,000-year record of East Asian monsoon rainfall from ^{10}Be in loess. *Science*, *360*(6391), 877–881. https://doi.org/10.1126/science.aam5825

Berger, A., & Loutre, M. (1991). Insolation values for the climate of the last 10 million years. *Quaternary Science Reviews*, *10*(4), 297–317. https://doi.org/10.1016/0277-3791(91)90033-q

Berger, A., Loutre, M. F., & Yin, Q. Z. (2010). Total irradiation during any time interval of the year using elliptic integrals. *Quaternary Science Reviews*, *29*(17–18), 1968–1982. https://doi.org/10.1016/j.quascirev.2010.05.007

Bosmans, J. H. C., Erb, M. P., Dolan, M. A., Drijthout, S. S., Tuenter, E., Hilgen, F. J., et al. (2018). Response of the Asian summer monsoons to idealized precession and obliquity forcing in a set of GCMs. *Quaternary Science Reviews*, *188*, 121–135. https://doi.org/10.1016/j.quascirev.2018.03.025

Caissie, B. E., Brigham-Greette, J., Cook, M. S., & Colmenero-Hidalgo, E. (2016). Bering Sea surface water conditions during marine isotope stages 12 to 10 at Navarin Canyon (IODP Site U1345). *Climate of the Past*, *12*(9), 1739–1763. https://doi.org/10.5194/cp-12-1739-2016

Chen, G., Zhang, P. F., & Lu, J. (2020). Sensitivity of the latitude of the westerly jet stream to climate forcing. *Geophysical Research Letters*, *47*(4), e2019GL086563. https://doi.org/10.1029/2019gl086563

Cheng, H., Edwards, R. L., Sinha, A., Spötl, C., Yi, L., Chen, S., et al. (2016). The Asian monsoon over the past 640,000 years and ice age terminations. *Nature*, *534*(7609), 640–646. https://doi.org/10.1038/nature18591

Cheng, L., Song, Y., Chang, H., Li, Y., Orozbaev, R., Zeng, M., & Liu, H. (2020). Heavy mineral assemblages and sedimentation rates of eastern Central Asian loess: Paleoenvironmental implications. *Palaeogeography, Palaeoclimatology, Palaeoecology*, *551*, 109747. https://doi.org/10.1016/j.palaeo.2020.109747

Cheng, L., Song, Y., Wu, Y., Liu, Y., Liu, H. F., Chang, H., et al. (2021). Drivers for asynchronous patterns of dust accumulation in central and eastern Asia and in Greenland during the Last Glacial Maximum. *Geophysical Research Letters*, *48*(5), e2020GL091194. https://doi.org/10.1029/2020gl091194

Cheng, T. Z., Zou, J. J., Shi, X. F., Gorbarenko, S., VasilenkoBosin, Y. A. Y., Bosin, A., et al. (2022). Climate-driven Changes in high-intensity wildfire on orbital timescales in Eurasia since 320 ka. *Lithosphere*, *9*, 7562666. https://doi.org/10.2113/2022/7562666

Chiang, J. C. H., Fung, I. Y., Wu, C. H., Cai, Y. J., Edman, J. P., Liu, Y. W., et al. (2015). Role of seasonal transitions and westerly jets in East Asian paleoclimate. *Quaternary Science Reviews*, *108*, 111–129. https://doi.org/10.1016/j.quascirev.2014.11.009

Chiang, J. C. H., Swenson, L. M., & Kong, W. (2017). Role of seasonal transitions and the westerlies in the interannual variability of the East Asian summer monsoon precipitation. *Geophysical Research Letters*, *44*(8), 3788–3795. https://doi.org/10.1002/2017GL072739

Clift, P. D., Wan, S. M., & Blusztajn, J. (2014). Reconstructing chemical weathering, physical erosion and monsoon intensity since 25Ma in the northern South China Sea: A review of competing proxies. *Earth-Science Reviews*, *130*, 86–102. https://doi.org/10.1016/j.earscirev.2014.01.002

de Menocal, P. B., Ortiz, J., Guilderson, T., Adkins, J., Sarnthein, M., Baker, L., & Yarusinsky, M. (2020). Abrupt onset and termination of the African humid period: Rapid climate responses to gradual insolation forcing. *Quaternary Science Reviews*, *19*(1–5), 347–361. https://doi.org/10.1016/s0277-3791(99)00081-5

Evan, A. T., Flamant, C., Gaetani, M., & Guichard, F. (2016). The past, present and future of African dust. *Nature*, *531*(7595), 493–495. https://doi.org/10.1038/nature17149

Fang, X. M., An, Z. S., Clemens, S. C., Zan, J. B., Shi, Z. G., Yang, S. L., & Han, W. X. (2020). The 3.6-Ma aridity and westerlies history over midlatitude Asia linked with global climatic cooling. *Proceedings of the National Academy of Sciences*, *117*(40), 24729–24734. https://doi.org/10.1073/pnas.1922710117

Gray, W. R., Wills, R. C. J., Rae, J. W. B., Burke, A., Ivanovic, R. F., Roberts, W. H. G., et al. (2020). Wind-driven evolution of the North Pacific subpolar gyre over the last deglaciation. *Paleoceanography and Paleoclimatology*, *47*(6), e2019GL086328. https://doi.org/10.1029/2019GL086328

Guo, B. H., Nie, J. S., Stevens, T., Buylaert, J. P., Peng, T. J., Xiao, W. J., et al. (2022). Dominant precessional forcing of the East Asian summer monsoon since 260 ka. *Geology*, *50*(12), 1372–1376. https://doi.org/10.1130/G50206.1

Guo, Z. T., Berger, A., Yin, Q. Z., & Qin, L. (2009). Strong asymmetry of hemispheric climates during MIS-13 inferred from correlating China loess and Antarctica ice records. *Climate of the Past*, *5*(1), 21–31. https://doi.org/10.5194/cp-5-21-2009

Han, Y. M., An, Z. S., Marlon, J. R., Bradley, R. S., Zhan, C. L., Arimoto, R., et al. (2020). Asian inland wildfires driven by glacial-interglacial climate change. *Proceedings of the National Academy of Sciences*, *117*(10), 5184–5189. https://doi.org/10.1073/pnas.1822035117

Herzschuh, U., Cao, X. Y., Laepple, T., Dallmeyer, A., Telford, R. J., Ni, J., et al. (2019). Position and orientation of the westerly jet determined holocene rainfall patterns in China. *Nature Communications*, *10*(1), 237. https://doi.org/10.1038/s41467-019-09866-8

Hovan, S. A., Rea, D. K., Pisias, N. J., & Shackleton, N. J. (1989). A direct link between the China loess and marine δ^{18}O records: aeolian flux to the North Pacific. *Nature*, *340*(6231), 296–298. https://doi.org/10.1038/340296a0

Huang, E., Wang, P., Wang, Y., Yan, M., Tian, J., Li, S. H., & Ma, W. T. (2020). Dole effect as a measurement of the low-latitude hydrological cycle over the past 800 ka. *Science Advances*, *6*(41), eaba4823. https://doi.org/10.1126/sciadv.aba4823

Jaccard, S. L., Galbraith, E. D., Sigman, D. M., & Haug, G. H. (2010). A pervasive link between Antarctic ice core and subarctic Pacific sediment records over the past 800 kyrs. *Quaternary Science Reviews*, *29*(1–2), 206–212. https://doi.org/10.1016/j.quascirev.2009.10.007

Jacobel, A. W., McManus, J. F., Anderson, R. F., & Winckler, G. (2017). Climate-related response of dust flux to the central equatorial Pacific over the past 150 kyr. *Earth and Planetary Science Letters*, *457*, 160–172. https://doi.org/10.1016/j.epsl.2016.09.042

Jickells, T. D., An, Z. S., Andersen, K. K., Baker, A. R., Bergametti, G., Brooks, N., et al (2005). Global iron connections between desert dust, ocean biogeochemistry, and climate. *Science*, *308*(5718), 67–71. https://doi.org/10.1126/science.1105959

Kanamitsu, M., Ebisuzaki, W., Woollen, J., Yang, S. K., Hnilo, J. J., Fiorino, M., & Potter, G. L. (2002). NCEP-DOE AMIP-II reanalysis (R-2). *Bulletin of the American Meteorological Society*, *83*(11), 1631–1643. https://doi.org/10.1175/bams-83-11-1631(2002)083<1631:nar>2.3.co;2

Kang, S. G., Wang, X. L., Du, J. H., & Song, Y. G. (2022). Paleoclimates inform on a weakening and amplitude-reduced East Asian winter monsoon in the warming future. *Geology*, *50*(11), 1224–1228. https://doi.org/10.1130/G50246.1

Kapp, P., Pelletier, J. D., Rohrmann, A., Heermance, R., Russell, J., & Ding, L. (2011). Wind erosion in the Qaidam basin, central Asia: Implications for tectonics, paleoclimate, and the source of the Loess Plateau. *Geological Society of America Today*, *21*(4/5), 4–10. https://doi.org/10.1130/gsatg99a.1

Kawahata, H., Okamoto, T., Matsumoto, E., & Ujiie, H. (2000). Fluctuations of eolian flux and ocean productivity in the mid-latitude North Pacific during the last 200 kyr. *Quaternary Science Reviews*, *19*(13), 1279–1291. https://doi.org/10.1016/S0277-3791(99)00096-7

Koffman, B. G., Yoder, M. F., Methven, T., Hanschka, L., Sears, H. B., Saylor, P. L., & Wallace, K. L. (2021). Glacial dust surpasses both volcanic ash and desert dust in its iron fertilization potential. *Global Biogeochemical Cycles*, *35*(4), e2020GB006821. https://doi.org/10.1029/2020gb006821

Kok, J. F., Storelvmo, T., Karydis, V. A., Adebiyi, A. A., Mahowald, N. M., Evan, A. T., et al. (2023). Mineral dust aerosol impacts on global climate and climate change. *Nature Reviews Earth and Environment*, *4*(2), 71–86. https://doi.org/10.1038/s43017-022-00379-5

Lamy, F., Chiang, J. C. H., Martínez-Méndez, G., Thierens, M., Arz, H. W., Bosmans, J., et al. (2019). Precession modulation of the South Pacific westerly wind belt over the past million years. *Proceedings of the National Academy of Sciences*, *116*(47), 23455–23460. https://doi.org/10.1073/pnas.1905847116

Larrasoaña, J., Roberts, A. P., Liu, Q. S., Lyons, R., Oldfield, F., Rohling, E. J., & Heslop, D. (2015). Source-to-sink magnetic properties of NE saharan dust in eastern mediterranean marine sediments: A review and paleoenvironmental implications. *Frontiers in Earth Science*, *3*. https://doi.org/10.3389/feart.2015.00019

Laskar, J., Robutel, P., Joutel, F., Gastineau, M., Correia, A. C. M., & Levrard, B. (2004). Long-term numerical solution for the insolation quantities of the Earth. *Astronomy and Astrophysics*, *428*(1), 261–285. https://doi.org/10.1051/0004-6361:20041335

Lee, S. Y., & Poulsen, C. J. (2009). Obliquity and precessional forcing of continental snow fall and melt: Implications for orbital forcing of pleistocene ice ages. *Quaternary Science Reviews*, *28*(25–26), 2663–2674. https://doi.org/10.1016/j.quascirev.2009.06.002

Lepre, C. J., & Olsen, P. E. (2021). Hematite reconstruction of late triassic hydroclimate over the colorado plateau. *Proceedings of the National Academy of Sciences*, *118*(7), e2004343118. https://doi.org/10.1073/pnas.2004343118

Li, G. Q., He, Y., Stevens, T., Zhang, X. J., Zhang, H. X., Wei, H. T., et al. (2020). Differential ice volume and orbital modulation of quaternary moisture patterns between Central and East Asia. *Earth and Planetary Science Letters*, *530*, 115901. https://doi.org/10.1016/j.epsl.2019.115901

Li, M., Hinnov, L., & Kump, L. (2019a). Acycle: Time-series analysis software for paleoclimate research and education. *Computers and Geosciences*, *127*, 12–22. https://doi.org/10.1016/j.cageo.2019.02.011

Li, Y., Song, Y., Qiang, M., Miao, Y. F., & Zeng, M. X. (2019b). Atmospheric dust variations in the Ili Basin, northwest China during the last glacial period as revealed by a high mountain loess-paleosol sequence. *Journal of Geophysical Research: Atmospheres*, *124*(15), 8449–8466. https://doi.org/10.1029/2019jd030470

Li, Y., Song, Y., Yin, Q. Z., Li, H., & Wang, Y. X. (2019c). Orbital and millennial northern mid-latitude westerlies over the last glacial period. *Climate Dynamics*, *53*(5–6), 3315–3324. https://doi.org/10.1007/s00382-019-04704-5

Limmer, D. R., Köhler, C. M., Hillier, S., Moreton, S. G., Tabrez, A. R., & Clift, P. D. (2012). Chemical weathering and provenance evolution of holocene–Recent sediments from the western indus shelf, northern Arabian Sea inferred from physical and mineralogical properties. *Marine Geology*, *326–328*, 101–115. https://doi.org/10.1016/j.margeo.2012.07.009

Lisiecki, L. E., & Raymo, M. E. (2005). A Pliocene-Pleistocene stack of 57 globally distributed benthic δ^{18}O records. *Paleoceanography*, *20*(1), PA1003. https://doi.org/10.1029/2004pa001071

Liu, Q. S., Roberts, A. P., Larrasonan, J. C., Banerjee, S. K., Guyodo, Y., Tauxe, L., & Oldfield, F. (2012). Environmental magnetism: Principles and applications. *Reviews of Geophysics*, *50*(4), RG4002. https://doi.org/10.1029/2012rg000393

Liu, Q. S., Sun, Y. B., Qiang, X. K., Tada, R. J., Hu, P. X., Duan, Z. Q., et al. (2015). Characterizing magnetic mineral assemblages of surface sediments from major Asian dust sources and implications for the Chinese loes magnetism. *Earth, Planets and Space*, *67*(1), 61. https://doi.org/10.1186/s40623-015-0237-8

Liu, W. G., Liu, Z. H., Sun, J. M., Song, C. H., Chang, H., Wang, H. Y., et al. (2020). Onset of permanent Taklimakan Desert linked to the mid-pleistocene transition. *Geology*, *48*(8), 782–786. https://doi.org/10.1130/g47406.1

Liu, Y. G., Zhong, Y., Gorbarenko, S. A., Boshi, A. A., Gong, X., Liu, Z. H., et al. (2022). High- and low-latitude forcing on the subarctic Pacific environment and productivity over the past 230 kyr. *Marine Geology*, *451*, 106875. https://doi.org/10.1016/j.margeo.2022.106875

Lohmann, G., Butzin, M., Eissner, N., Shi, X. X., & Stepanek, C. (2020). Abrupt climate and weather changes across time scales. *Paleoceanography and Paleoclimatology*, *35*(9), e2019PA003782. https://doi.org/10.1029/2019PA003782

Lu, J., Chen, G., & Frierson, D. M. W. (2010). The position of the midlatitude storm track and eddy-driven westerlies in aquaplanet AGCMs. *Journal of the Atmospheric Sciences*, *67*(12), 3984–4000. https://doi.org/10.1175/2010jas3477.1

Lund, S., Mortazavi, E., Platman, E., Kirby, M., Stoner, J., & Okada, M. (2021). Rock magnetic variability of quaternary deep-sea sediments from the Bering Sea and their environmental implications. *Deep Sea Research Part I: Oceanographic Research Papers*, *172*, 103487. https://doi.org/10.1016/j.dsr.2021.103487

Lüthi, D., Le Floch, M., Bereiter, B., Blunier, T., Barnola, J., Siegenthaler, U., et al. (2008). High-resolution carbon dioxide concentration record 650,000-800,000 years before present. *Nature*, *453*(7193), 379–382. https://doi.org/10.1038/nature06949

Lyu, A. Q., & Yin, Q. Z. (2022). The spatial-temporal patterns of East Asian climate in response to insolation, CO_2 and ice sheets during MIS-5. *Quaternary Science Reviews*, *293*, 10768. https://doi.org/10.1016/j.quascirev.2022.107689

Lyu, A. Q., Yin, Q. Z., Crucifix, M., & Sun, Y. B. (2021). Diverse regional sensitivity of summer precipitation in East Asia to ice volume, CO_2 and astronomical forcing. *Geophysical Research Letters*, *48*(7), e2020GL092005. https://doi.org/10.1029/2020GL092005

Maher, B. A. (2011). The magnetic properties of quaternary aeolian dusts and sediments, and their palaeoclimatic significance. *Aeolian Research*, *3*(2), 87–144. https://doi.org/10.1016/j.aeolia.2011.01.005

Maher, B. A., Prospero, J. M., Gaiero, D., Hesse, P. P., & Balkanski, Y. (2010). Global connections between aeolian dust, climate and ocean biogeochemistry at the present day and at the last glacial maximum. *Earth-Science Reviews*, *99*(1–2), 61–97. https://doi.org/10.1016/j.earscirev.2009.12.001

Mantsis, D. F., Lintner, B. R., BroccoliA, J., Erb, M. P., Clement, A. C., & Park, H. S. (2014). The response of large-scale circulation to obliquity-induced changes in meridional heating gradients. *Journal of Climate*, *27*(14), 5504–5516. https://doi.org/10.1175/jcli-d-13-00526.1

Mao, R., Ho, C. H., Shao, Y. P., Gong, D. Y., & Kim, J. (2011). Influence of Arctic oscillation on dust activity over northeast Asia. *Atmospheric Environment*, *45*(2), 326–337. https://doi.org/10.1016/j.atmosenv.2010.10.020

Martin, J. H. (1990). Glacial-interglacial CO_2 change, the iron hypothesis. *Paleoceanography*, *5*, 1–13. https://doi.org/10.1029/pa005i001p00001

Mayaud, J. R., Wiggs, G. F. S., & Bailey, R. M. (2016). Characterizing turbulent wind flow around dryland vegetation. *Earth Surface Processes and Landforms*, *41*(10), 1421–1436. https://doi.org/10.1002/esp.3934

Moore, C. M., Mills, M. M., Arrigo, K. R., Berman-Frank, I., Bopp, L., Boyd, P. W., et al. (2013). Processes and patterns of oceanic nutrient limitation. *Nature Geoscience*, *6*(9), 701–710. https://doi.org/10.1038/ngeo1765

Nagashima, K., Tada, R., Matsui, H., Irino, T., Tani, A., & Toyoda, S. (2007). Orbital- and millenial-scale variations in asian dust transport path to the Japan Sea. *Palaeogeography, Palaeoclimatology, Palaeoecology*, *247*(1–2), 144–161. https://doi.org/10.1016/j.palaeo.2006.11.027

Nagashima, K., Tada, R., Tani, A., Sun, Y. B., Isozaki, Y., Yoyoda, S., & Hasegawa, H. (2011). Millennial-scale oscillations of the westerly jet path during the last glacial period. *Journal of Asian Earth Sciences*, *40*(6), 1214–1220. https://doi.org/10.1016/j.jseaes.2010.08.010

Nwaodua, E. C., Ortiz, J. D., & Griffith, E. M. (2014). Diffuse spectral reflectance of surficial sediments indicates sedimentary environments on the shelves of the Bering Sea and western Arctic. *Marine Geology*, *355*(3), 218–233. https://doi.org/10.1016/j.margeo.2014.05.023

Oldfield, F., Chiverrell, R. C., Lyons, R., Williams, E., Shen, Z., Bristow, C., et al. (2014). Discriminating dusts and dusts sources using magnetic properties and hematite: Goethite ratios of surface materials and dust from North Africa, the Atlantic and Barbados. *Aeolian Research*, *13*, 91–104. https://doi.org/10.1016/j.aeolia.2014.03.010

Ortiz, J. D., Polyak, L., Grebmeier, J. M., Darby, D., Eberl, D. D., Naidu, S., & Nof, D. (2009). Provenance of holocene sediment on the Chukchi-Alaskan margin based on combined diffuse spectral reflectance and quantitative X-Ray diffraction analysis. *Global and Planetary Change*, *68*(1–2), 73–84. https://doi.org/10.1016/j.gloplacha.2009.03.020

Serno, S., Winckler, G., Anderson, R. F., Hayes, C. T., McGee, D., Machalett, B., et al. (2014). Eolian dust input to the subarctic North Pacific. *Earth and Planetary Science Letters*, *387*, 252–263. https://doi.org/10.1016/j.epsl.2013.11.008

Serno, S., Winckler, G., Anderson, R. F., Jaccard, S. L., Kienast, S. S., Haug, G. H., *et al.* (2017). Change in dust seasonality as the primary driver for orbital-scale dust storm variability in East Asia. *Geophysical Research Letters*, *44*(8), 3796–3805. https://doi.org/10.1002/2016gl072345

Shao, Y. P., Wyrwoll, K. H., Chappell, A., Huang, J. P., Liu, Z. H., McTainshi, G. H., et al. (2011). Dust cycle: An emerging core theme in Earth system science. *Aeolian Research*, *2*(4), 181–204. https://doi.org/10.1016/j.aeolia.2011.02.001

Shaw, T. A., Baldwin, M., Barnes, E. A., Caballero, R., Garfinkel, C. I., Hwang, Y. T., et al. (2016). Storm track processes and the opposing influences of climate change. *Nature Geoscience*, *9*, 656–664. https://doi.org/10.1038/ngeo2783

Shi, X. X., Lohmann, G., Sidorenko, D., & Yang, H. (2020). Early-Holocene simulations using different forcings and resolutions in AWI-ESM. *The Holocene*, *30*(7), 996–1015. https://doi.org/10.1177/0959683620908634

Sidorenko, D., Goessling, H. F., Koldunov, N. V., Scholz, P., Danilov, S., Barbi, D., et al. (2019). Evaluation of FESOM2.0 coupled to ECHAM6.3: Preindustrial and HighResMIP simulations. *Journal of Advances in Modeling Earth Systems*, *11*, 3794–3815. https://doi.org/10.1029/2019ms001696

Skonieczny, C., McGee, D., Winckler, G., Bory, A., Bradtmiller, L. I., Kinsley, C. W., et al. (2019). Monsoon-driven saharan dust variability over the past 240,000 years. *Science Advances*, *5*(1), eaav1887. https://doi.org/10.1126/sciadv.aav1887

Sun, Y. B., Yin, Q. Z., Crucifix, M., Clemens, S. C., Araya-Melo, P., Liu, W. G., et al. (2019). Diverse manifestations of the mid-pleistocene climate transition. *Nature Communications*, *10*(1), 352. https://doi.org/10.1038/s41467-018-08257-9

Szopa, S., et al. (2021). Short-lived climate forcers. In V. Masson-Delmotte, P. Zhai, A. Pirani, S. L. Connors, C. Péan, S. Berger, et al. (Eds.), *Climate change 2021: The physical science basis. Contribution of working group I to the sixth assessment report of the intergovernmental panel on climate change* (pp. 817–922). Cambridge University Press.

Tagliabue, A., Bowie, A. R., Bord, P. W., Buck, K. N., Johnson, K. S., & Saito, M. A. (2017). The integral role of iron in ocean biogeochemistry. *Nature*, *543*(7643), 51–59. https://doi.org/10.1038/nature21058

Tierney, J. E., de Menocal, P. B., & Zander, P. D. (2017). A climate context for the out-of-Africa migration. *Geology*, *45*(11), 1023–1026. https://doi.org/10.1130/G39457.1

Timmermann, A., Friedrich, T., Timm, O. E., Chikamoto, M. O., Abe-Ouchi, A., & Ganopolski, A. (2014). Modeling obliquity and CO_2 effects on Southern Hemisphere climate during the past 408 ka. *Journal of Climate*, *27*(5), 1863–1875. https://doi.org/10.1175/jcli-d-13-00311.1

Újvári, G., Stevens, T., Molnár, M., Demény, A., Lambert, F., Varga, G., et al. (2017). Coupled european and greenland last glacial dust activity driven by North Atlantic climate. *Proceedings of the National Academy of Sciences*, *114*(50), 10632–10638. https://doi.org/10.1073/pnas.1712651114

Uno, I., Eguchi, K., Yumimoto, K., Takemura, T., Shimizu, A., Uematsu, M., et al. (2009). Asian dust transported one full circuit around the globe. *Nature Geoscience*, *2*(8), 557–560. https://doi.org/10.1038/ngeo583

Wang, P. X. (2021). Low-latitude forcing: A new insight into paleo-climate changes. *The Innovation*, *2*(3), 100145. https://doi.org/10.1016/j.xinn.2021.100145

Weber, E. T., Owen, R. M., Kent-Corson, G. R., Halliday, A. N., Jones, C. E., & Rea, D. K. (1996). Quantitative resolution of eolian continental crustal material and volcanic detritus in the North Pacific surface sediment. *Paleoceanography*, *2*, 115–127.

Wu, C., Lin, Z., Shao, Y., Liu, X., & Li, Y. (2022). Drivers of recent decline in dust activity over East Asia. *Nature Communications*, *13*(1), 7105. https://doi.org/10.1038/s41467-022-34823-3

Xie, X., Liu, X., Chen, G., & Korty, R. L. (2019). A transient modeling study of the latitude dependence of East Asian winter monsoon variations on orbital timescales. *Geophysical Research Letters*, *46*(13), 7565–7573. https://doi.org/10.1029/2019gl083060

Xu, Z. K., Li, T. G., Clift, P. D., Lim, D., Wan, S. M., Chen, H. J., et al. (2015). Quantitative estimates of Asian dust input to the western Philippine Sea in the mid-late quaternary and its potential significance for paleoenvironment. *Geochemistry, Geophysics, Geosystems*, *16*(9), 3182–3196. https://doi.org/10.1002/2015GC005929

Yamazaki, Y. (2009). Environmental magnetism of pleistocene sediments in the North Pacific and Ontong-Java Plateau: Temporal variations of detrital and biogenic components. *Geochemistry, Geophysics, Geosystems*, *10*(7), Q07Z04. https://doi.org/10.1029/2009gc002413

Yang, H., Lohmann, G., Lu, J., Gowan, E. J., Shi, X. X., Liu, J. P., & Wang, Q. (2020). Tropical expansion driven by poleward advancing midlatitude meridional temperature gradients. *Journal of Geophysical Research-Atmospheres*, *125*(16), e2020JG033158. https://doi.org/10.1029/2020JD033158

Yang, X., Zhou, C., Zhou, W., Yang, F., Liu, X., & Mamtimin, A. (2019). A study on the effects of soil moisture, air humidity, and air temperature on wind speed threshold for dust emissions in the Taklimakan Desert. *Natural Hazards*, *97*(3), 1069–1081. https://doi.org/10.1007/s11069-019-03686-1

Yao, Z. Q., Liu, Y. G., Shi, X. F., Gong, X., Gorbarenko, S. A., Bosin, A. A., et al. (2022). Paleoproductivity variations and implications in the subarctic northwestern Pacific since MIS 7: Geochemical evidence. *Global and Planetary Change*, *209*, 103730. https://doi.org/10.1016/j.gloplacha.2021.103730

Yin, Q. Z. (2013). Insolation-induced mid-brunhes transition in Southern Ocean ventilation and deep-ocean temperature. *Nature*, *494*(7436), 222–225. https://doi.org/10.1038/nature11790

Zhang, P., Xu, J., Holbourn, A. W., Kuhnt, W., Xiong, Z. F., & Li, T. G. (2022). Obliquity induced latitudinal migration of the intertropical convergence zone during the past ~410 kyr. *Geophysical Research Letters*, *49*(21), 2022GL100039. https://doi.org/10.1029/2022GL100039

Zhang, Q., Liu, Q. S., Li, J. H., & Sun, Y. B. (2018). An integrated study of the eolian dust in pelagic sediments from the North Pacific Ocean based on environmental magnetism, transmission electron microscopy and diffuse reflectance spectroscopy. *Journal of Geophysical Research: Solid Earth*, *122*(5), 3358–3376. https://doi.org/10.1002/2017jb014951

Zhang, Q., Liu, Q. S., Roberts, A. P., Larrasoaña, J. C., Shi, X. F., & Jin, C. S. (2020). Mechanism for enhanced eolian dust flux recorded in North Pacific Ocean sediments since 4.0 Ma: Aridity or humidity at dust source areas in the Asian interior? *Geology*, *48*(1), 77–81. https://doi.org/10.1130/g46862.1

Zhang, W. F., Chen, J., Ji, J. F., & Li, G. J. (2016). Evolving flux of asian dust in the North Pacific Ocean since the late oligocene. *Aeolian Research*, *23*, 11–20. https://doi.org/10.1016/j.aeolia.2016.09.004

Zhang, Y. C., Kuang, X. Y., Guo, W. D., & Zhou, T. J. (2006). Seasonal evolution of the upper-tropospheric westerly jet core over East Asia. *Geophysical Research Letters*, *33*(11), L11708. https://doi.org/10.1029/2006gl026377

Zhao, Y., Wang, M. Z., Huang, A. N., Li, H. J., Huo, W., & Yang, Q. (2014). Relationships between the West Asian subtropical westerly jet and summer precipitation in northern Xinjiang. *Theoretical and Applied Climatology*, *116*(3–4), 403–411. https://doi.org/10.1007/s00704-013-0948-3

Zhong, Y., Liu, Y. G., Gong, X., Wilson, D. J., Lu, Z. Y., Liu, J. B., et al. (2021). Coupled impacts of atmospheric circulation and sea-ice on late pleistocene terrigenous sediment dynamics in the Subarctic Pacific Ocean. *Geophysical Research Letters*, *48*(19), e2021GL095312. https://doi.org/10.1029/2021GL095312

Zhong, Y., Liu, Y. G., Yang, X. Q., Zhang, J., Liu, J. B., Bosin, A., et al. (2020). Do non-dipole geomagnetic field behaviors persistently exist in the subarctic Pacific Ocean over the past 140 ka? *Science Bulletin*, *65*(18), 1505–1507. https://doi.org/10.1016/j.scib.2020.05.016

Zhong, Y., Shi, X. F., Yang, H., Wilson, D. J., Hein, J. R., Kaboth-Bahr, S., et al. (2022). Humidification of Central Asia and equatorward shifts of westerly winds since the late pliocene. *Communications Earth & Environment*, *3*(1), 274. https://doi.org/10.1038/s43247-022-00604-5

References From the Supporting Information

Bailey, J. C. (1993). Geochemical history of sediments in the northwestern Pacific Ocean. *Geochemical Journal*, *27*(2), 71–90. https://doi.org/10.2343/geochemj.27.71

Barker, S., Knorr, G., Edward, R. L., Parrenin, F., Putnam, A. E., Skinner, L. C., et al. (2011). 800,000 years of abrupt climate variability. *Science*, *334*(6054), 347–351. https://doi.org/10.1126/science.1203580

Hovan, S. A., Rea, D. K., & Pisias, N. G. (1991). Late pleistocene continental climate and oceanic variability recorded in northwest pacific sediments. *Paleoceanography*, *6*(3), 349–370. https://doi.org/10.1029/91PA00559

Jaccard, S. L., Galbraith, E. D., Sigman, D. M., Haug, G. H., Francois, R., Pedersen, T. F., et al. (2009). Subarctic Pacific evidence for a glacial deepening of the oceanic respired carbon pool. *Earth and Planetary Science Letters*, *277*(1), 156–165. https://doi.org/10.1016/j.epsl.2008.10.017

Kinsley, C. W., Bradtmiller, L. I., Zhang, Y., Perala-Dewey, J., & McGee, D. (2022). Ocean-atmosphere changes in the midlatitude North Pacific over the last 330 ka: Dust, biogenic sediment and authigenic uranium accumulation at Shatsky Rise. (Version 1) [Dataset]. Zenodo. https://doi.org/10.5281/zenodo.6791725

Lambert, F., Delmonte, B., Petit, J. R., Bigler, M., Kaufmann, P. R., Hutterli, M. A., et al. (2008). Dust-climate couplings over the past 800,000 years from the EPICA Dome C ice core. *Nature*, *452*(7187), 616–619. https://doi.org/10.1038/nature06763

Liu, Y., Lo, L., Shi, Z. G., Wei, K. Y., Chou, C. J., Chen, Y. C., et al. (2015). Obliquity pacing of the western pacific intertropical convergence zone over the past 282,000 years. *Nature Communications*, *6*(1), 10018. https://doi.org/10.1038/ncomms10018

Lu, Z. Y., Liu, Z. Y., Chen, G. S., & Guan, J. (2019). Prominent precession band variance in ENSO intensity over the last 300,000 years. *Geophysical Research Letters*, *46*(16), 9786–9795. https://doi.org/10.1029/2019gl083410

Martínez-Garcia, A., Rosell-Melé, A., Jaccard, S. L., Geibert, W., Sigman, D. M., & Haug, G. H. (2011). Southern Ocean dust-climate coupling over the past four million years. *Nature*, *476*(7360), 312–315. https://doi.org/10.1038/nature10310

Scheinost, A. C., Chavernas, A., Barrón, V., & Torren, J. (1998). Use and limitations of second-derivative diffuse reflectance spectroscopy in the visible to near-infrared range to identify and quantify Fe oxide minerals in soils. *Clays and Clay Minerals*, *46*(5), 528–536. https://doi.org/10.1346/CCMN.1998.0460506

Torrent, J., Liu, Q. S., Bloemendal, J., & Barron, V. (2007). Magnetic enhancement and iron oxides in the upper luochuan loess-paleosol sequence, Chinese loess plateau. *Soil Science Society of America Journal*, *71*(5), 1570–1578. https://doi.org/10.2136/sssaj2006.0328

Winckler, G., Anderson, R. F., Fleisher, M. Q., Mcgee, D., & Mahowald, N. (2008). Covariant glacial-interglacial dust fluxes in the equatorial Pacific and Antarctica. *Science*, *320*(5872), 93–96. https://doi.org/10.1126/science.1150595

Yang, H., Lohmann, G., Krebs-Kanzow, U., Ionita, M., Shi, X. X., Sidorenko, D., et al. (2020). Poleward shift of the major ocean gyres detected in a warming climate. *Geophysical Research Letters*, *47*(5), e2019GL085868. https://doi.org/10.1029/2019GL085868

Yeager, S. G., Shields, C. A., Large, W. G., & Hack, J. J. (2006). The low-resolution CCSM3. *Journal of Climate*, *19*(11), 2545–2566. https://doi.org/10.1175/jcli3744.1

Zhang, P., Xu, J., Holbourn, A., Kunhnt, W., Beil, S., Li, T. G., et al. (2020). Indo-pacific hydroclimate in response to changes of the intertropical convergence zone: Discrepancy on precession and obliquity bands over the last 410 kyr. *Journal of Geophysical Research: Atmospheres*, *125*(14), e2019JD032125. https://doi.org/10.1029/2019JD032125

Ziegler, C. L., Murray, R. W., Hovan, S. A., & Rea, D. K. (2007). Resolving eolian, volcanogenic, and authigenic components in pelagic sediments from the Pacific Ocean. *Earth and Planetary Science Letters*, *254*(3), 416–432. https://doi.org/10.1016/j.epsl.2006.11.049